

Defect selective passivation in GaN epitaxial growth and its application to light emitting diodes

M.-H. Lo, P.-M. Tu, C.-H. Wang, Y.-J. Cheng, C.-W. Hung, S.-C. Hsu, H.-C. Kuo, H.-W. Zan, S.-C. Wang, C.-Y. Chang, and C.-M. Liu

Citation: *Applied Physics Letters* **95**, 211103 (2009); doi: 10.1063/1.3266859

View online: <http://dx.doi.org/10.1063/1.3266859>

View Table of Contents: <http://scitation.aip.org/content/aip/journal/apl/95/21?ver=pdfcov>

Published by the *AIP Publishing*

Articles you may be interested in

[GaN light-emitting diodes using separate epitaxial growth for the p-type region to attain polarization-inverted electron-blocking layer, reduced electron leakage, and improved hole injection](#)

Appl. Phys. Lett. **103**, 201112 (2013); 10.1063/1.4829576

[Near milliwatt power AlGaIn-based ultraviolet light emitting diodes based on lateral epitaxial overgrowth of AlN on Si\(111\)](#)

Appl. Phys. Lett. **102**, 011106 (2013); 10.1063/1.4773565

[A visualization of threading dislocations formation and dynamics in mosaic growth of GaN-based light emitting diode epitaxial layers on \(0001\) sapphire](#)

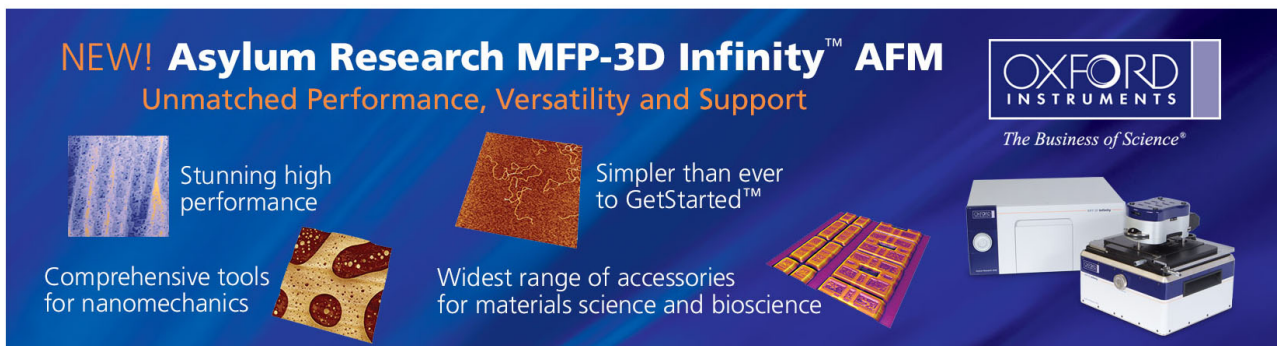
Appl. Phys. Lett. **101**, 231911 (2012); 10.1063/1.4769905

[Defect reduction and efficiency improvement of near-ultraviolet emitters via laterally overgrown GaN on a GaN/patterned sapphire template](#)

Appl. Phys. Lett. **89**, 161105 (2006); 10.1063/1.2363148

[Influence of residual oxygen impurity in quaternary InAlGaIn multiple-quantum-well active layers on emission efficiency of ultraviolet light-emitting diodes on GaN substrates](#)

J. Appl. Phys. **99**, 114509 (2006); 10.1063/1.2200749



NEW! Asylum Research MFP-3D Infinity™ AFM
Unmatched Performance, Versatility and Support

OXFORD INSTRUMENTS
The Business of Science®

Stunning high performance
Simpler than ever to GetStarted™

Comprehensive tools for nanomechanics
Widest range of accessories for materials science and bioscience

Defect selective passivation in GaN epitaxial growth and its application to light emitting diodes

M.-H. Lo,^{1,2} P.-M. Tu,¹ C.-H. Wang,¹ Y.-J. Cheng,^{1,2,a)} C.-W. Hung,¹ S.-C. Hsu,² H.-C. Kuo,¹ H.-W. Zan,¹ S.-C. Wang,¹ C.-Y. Chang,³ and C.-M. Liu⁴

¹Department of Photonics and Institute of Electro-Optical Engineering, National Chiao Tung University, 1001 Ta Hsueh Rd., Hsinchu 300, Taiwan

²Research Center for Applied Sciences, Academia Sinica, Taipei 11529, Taiwan

³Institute of Electronics, National Chiao Tung University, 1001 Ta Hsueh Rd., Hsinchu 300, Taiwan

⁴Sino-American Silicon Products Inc., Hsinchu 300, Taiwan

(Received 4 August 2009; accepted 28 October 2009; published online 24 November 2009)

A defect selective passivation method to block the propagation of threading dislocations in GaN epitaxial growth is demonstrated. The defect selective passivation is done by using defect selective chemical etching to locate defect sites, followed by silicon oxide passivation of the etched pits, and epitaxial over growth. The threading dislocation density in the regrown epilayer is significantly improved from 1×10^9 to 4×10^7 cm⁻². The defect passivated epiwafer is used to grow light emitting diode and the output power of the fabricated chip is enhanced by 45% at 20 mA compared to a reference one without using defect passivation. © 2009 American Institute of Physics. [doi:10.1063/1.3266859]

GaN based light emitting devices have attracted great attention in last few years due to its importance in solid state lighting applications. Researchers are actively investigating various approaches to improve device performance. The devices are often epitaxially grown on foreign substrates, for example sapphire. The as grown GaN epitaxial layer has high threading dislocation (TD) density typically in the range of 10^8 – 10^{10} cm⁻² due to the mismatches in lattice constants and thermal expansion coefficients between GaN and sapphire. These defects are nonradiative recombination centers and are detrimental to optoelectronic device performance. The reduction of TD is of great importance for the development of GaN based devices.

There are several epitaxial growth methods to improve crystal quality. A very commonly used one is the epitaxial lateral overgrowth technique (ELOG).^{1,2} Strips of SiO₂ mask along specific crystal direction are deposited on GaN epilayer, followed by epitaxial growth. The growth starts from the window regions and grows vertically as well as laterally to cover the SiO₂ strips until obtaining planar surface over whole wafer. The lateral growth above mask area bends the propagation direction of threading dislocation and results in significantly lower defect density. The defect density is however still high at window regions and coalescent boundaries. Another approach is to use patterned sapphire substrate for epitaxial growth,^{3,4} but the reduction in TD defect density is often not as effective as ELOG method. Other methods use *in situ* SiN_x or *ex situ* TiN_x porous insertion layers,^{5,6} where GaN nucleates from the pores of the inserted layer and lateral overgrowth on top of it. Recently, defect reduction methods using defect selective etching followed by metalorganic chemical vapor deposition (MOCVD)⁷ or hydride vapor phase epitaxy⁸ regrowth have also been reported. In this letter, we demonstrate a TD reduction method by self-aligned defect selective passivation without the need of photolithography and use it to fabricate a high efficiency light emitting

diodes (LED). The defect selective passivation is done by defect selective etching, SiO₂ passivation at etch pits, and epitaxial over growth.

The schematic of process flow is shown in Figs. 1(a)–1(d). A 30 nm of low temperature GaN nucleation layer followed by a 2 μm GaN buffer layer is grown on (0001) sapphire template by low pressure MOCVD. The GaN wafer is immersed in high temperature molten KOH at 280 °C for 10 min. The molten KOH selectively etches defect sites and forms hexagonal pits on GaN surface⁹ as illustrated in Fig. 1(a). There can be one or several TDs under an etch pit and the KOH etching may not etch all defects, which will be explained later. A 0.5 μm SiO₂ film is deposited on the etched surface by plasma enhanced chemical vapor deposition as shown in Fig. 1(b). The SiO₂ thin film on the flat surface area is then removed by chemical mechanical polishing, which leaves only SiO₂ at the etched pits as shown in Fig. 1(c). The SiO₂ fillings at etch pits act as defect passivation to block the continuous propagation of TDs in the subsequent epitaxial growth. The exposed GaN flat surface provides the seed layer for epitaxial regrowth, which grows in

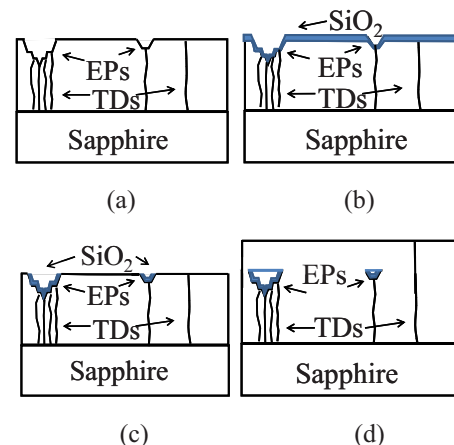


FIG. 1. (Color online) [(a)–(d)] Defect selective passivation process flow.

^{a)}Electronic mail: yjcheng@sinica.edu.tw.

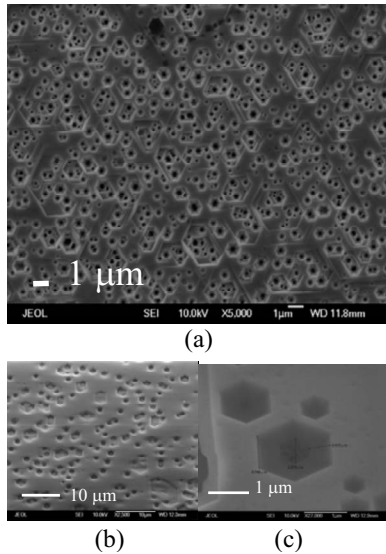


FIG. 2. [(a)–(c)] SEM image of the sample surface corresponding to the process step in Figs. 1(a)–1(c), respectively.

both vertical and lateral direction to cover over the SiO_2 passivated pits, as shown in Fig. 1(d). This defect passivation and regrowth process can be viewed as a variation of conventional ELOG method but with some unique advantages. First, photolithography patterning is not required. Second, micro SiO_2 masks are self-aligned to the TD pits created by defect selective etching. Third, the size of each mask is exactly matched to individual etch pit size. This method, compared to ELOG, provides defect selective passivation rather than random blocking of TD defects.

Figures 2(a)–2(c) are the surface scanning electron microscope (SEM) images corresponding to processing steps Figs. 1(a)–1(c). Figure 2(a) shows the random distribution of hexagonal pits after molten KOH etching. The etched crystal planes are mostly $\{1\bar{1}01\}$ facets. Aside from individual hexagonal pits, there are often several pits clustered together. The etch pit density counting all the individual pits is about $5 \times 10^8 \text{ cm}^{-2}$. The deposited SiO_2 thin film follows the etched pit topography as shown in Fig. 2(b). After chemical mechanical polishing (CMP) process, only SiO_2 in etched pits are left as shown in Fig. 2(c). Small pits are filled with SiO_2 . For large pits, SiO_2 only fills the side walls leaving a void in the center. The subsequent MOCVD epitaxial overgrowth covers the whole wafer with flat surface. A LED structure with $2 \mu\text{m}$ Si-doped n-GaN, ten pairs of InGaN/GaN multiple quantum wells (QWs), and a 30 nm Mg-doped p-GaN were grown on the template. The QW emission wavelength is at 425 nm.

To assess the TD reduction, a tunneling electron microscope (TEM) image was taken as shown in Fig. 3(a). The TD density can be estimated by directly counting the TD lines in the plane-view micrograph. The TD density estimated at the dashed line right below defect passivation layer is about $1 \times 10^9 \text{ cm}^{-2}$. This number is slightly larger than the KOH etch pit density $5 \times 10^8 \text{ cm}^{-2}$. The discrepancy is due to the fact that there can be multiple TDs under an etch pit as can be seen in Fig. 3(a). The TD density is significantly reduced to $4 \times 10^7 \text{ cm}^{-2}$ at the dashed line near the QW region. SiO_2 passivations at etched pits do effectively block the propagation of TDs. The SEM image however also shows that SiO_2 fillings do not occur on top of all TDs. In other words, not all

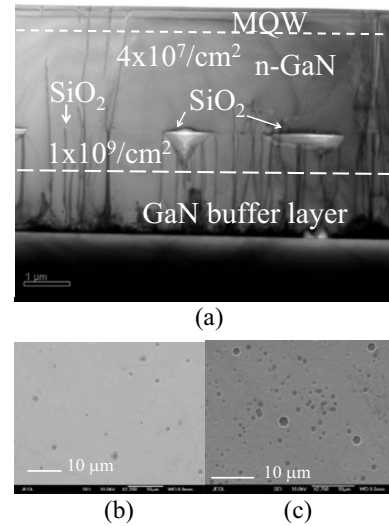


FIG. 3. (a) TEM image of LED sample with defect selective passivation. (b) SEM image of the defect passivated sample after molten KOH etching. (c) SEM image of the defect passivated sample after high temperature H_3PO_4 etching.

the TDs are etched by molten KOH. As a result, some TDs are not blocked and propagate all the way to the top surface. Those TDs not etched by KOH are presumably specific types of TDs resistive to molten KOH etching. It has been reported that KOH preferentially etches screw type TD and is less effective in etching edge and mixed type TDs.¹⁰ To verify if those TDs propagating all the way to the top surface are resistive to KOH etching, the regrown sample was put in molten KOH under the same etching conditions again. The SEM image of the etched sample is shown in Fig. 3(b). There are much less etch pits, with density of only $1 \times 10^5 \text{ cm}^{-2}$. The great reduction in etch pit density from 5×10^8 to $1 \times 10^5 \text{ cm}^{-2}$ shows that the TDs that can be etched by KOH are mostly blocked by the SiO_2 fillings in the defect selective passivation process. The etch pit density $1 \times 10^5 \text{ cm}^{-2}$ is much smaller than the TD density $4 \times 10^7 \text{ cm}^{-2}$ estimated from the cross section TEM image near surface region. Most of TDs not blocked by defect passivation process are those resistive to KOH etching. The sample was subsequently immersed in 195°C H_3PO_4 solution for 20 min. It has been reported that KOH and H_3PO_4 have different preferential crystallographic etch planes.¹¹ The surface SEM image is shown in Fig. 3(c). The H_3PO_4 etch pit morphology is very different from that of KOH etching. The etch pit density is about $1.2 \times 10^7 \text{ cm}^{-2}$. This number is close to the TD density estimated from the TEM image near surface region. This implies that KOH and H_3PO_4 somehow etches different defect types of TDs and both should probably be used to etch TDs in the defect selective etching process to increase defect passivation coverage.

The optical characteristic is investigated by cathodoluminescent (CL) and SEM cross section images as shown in Figs. 4(a) and 4(b). These two images are taken by simply switching detection mode from cathodoluminescent detection to scattering electron detection under the same magnification condition and thus have one to one location correspondence. The CL intensity changes dramatically across SiO_2 passivation boundary. The bright CL spots are mostly located at the regrown GaN right on top of SiO_2 passivation masks. The intensity of bright CL spot is so high that when it

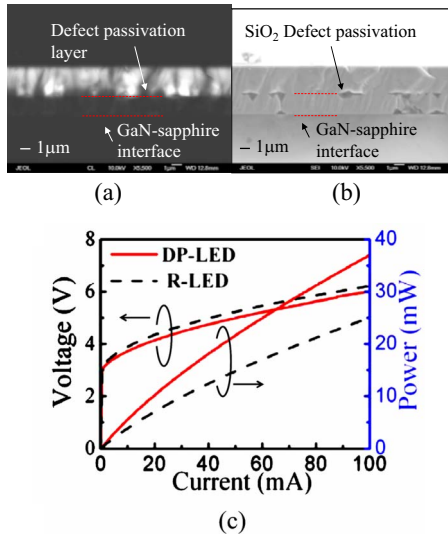


FIG. 4. (Color online) [(a) and (b)] Cross section CL and SEM image of the defect passivated epi-wafer under same magnification. (c) L-I and V-I curve of the DP-LED and R-LED.

is adjusted not to saturate detector, the CL intensity difference between lower GaN layer and sapphire become visually hard to distinguish. By analyzing the gray scale levels of image pixels, we can still identify GaN-sapphire interface, which is also confirmed by comparing Figs. 4(a) and 4(b). The CL intensity averaged over the cross section area of the regrown layer is measured to be about 23 times of that of the layer below passivation boundary. The threading dislocation defects are strong nonradiative recombination centers.¹² The significant increase in CL intensity demonstrates that the loss of excited carriers due to nonradiative recombination is greatly reduced in the defect passivated layer as a result of the reduction in TD density.

LED chips with size of $300 \times 300 \mu\text{m}^2$ were fabricated from the defect passivated epiwafer. The optical and electrical characteristics are compared with a reference LED going through the same fabrication process except for the defect passivation layer. The light current (L-I) and voltage current (V-I) curves of the defect passivated LED (DP-LED) and reference LED (R-LED) are shown in Fig. 4(c). The driving voltage of DP-LED (red solid line) is slightly lower than that (black dotted line) of R-LED. We remark that this slightly lower driving voltage may be due to the lower defect density. When the defect density is lower, electrons are easier to move across material without scattering thus leading to lower resistance and driving voltage. The optical output power is however significantly enhanced by 45% compared to that of the reference sample at 20 mA. The SiO_2 masks not only block the propagation of TD but also can act as light scattering sites to improve LED light extraction efficiency, similar to the use of patterned GaN-sapphire interface^{3,13} to reduce light trapped by total internal reflection. A Monte Carlo ray tracing simulation is used to check if light extraction enhancement is a significant part of total output power

enhancement. A simplified two-dimensional array of inverted hexagonal pyramid SiO_2 masks is used to model the defect passivation. Various geometries with $0.7\text{--}1 \mu\text{m}$ lateral size, $0.5\text{--}1 \mu\text{m}$ height, and $3\text{--}4 \mu\text{m}$ center to center spacing are calculated and show a variation of light extraction enhancement from 10%–25%. It shows that light extraction enhancement cannot be totally neglected in the total 45% output power enhancement. The output power enhancement from TD defect reduction is not as large as the above measured CL intensity enhancement. It has been reported that InGaN quantum well emission is less sensitive to TD defects. LEDs using GaN or AlGaIn active layer is however very sensitive to TD defects and really requires the reduction of TD.^{14,15}

In summary, we have demonstrated a defect selective passivation method to reduce TD density and used it to fabricate a LED. The defect passivation SiO_2 masks are self-aligned to the TD defect pits created by KOH defect selective etching without photolithography patterning and can significantly reduce TD density from 1×10^9 to $4 \times 10^7 \text{ cm}^{-2}$. The SiO_2 masks also improve the light extraction efficiency in LED application. TEM image shows that some defects are resistive to KOH etching and propagate all the way to the top surface. Further improvement can be made by exploring additional etching chemicals that are complementary to KOH in defect selective etching to increase the coverage rate of defect selective passivation.

This work was financially supported by Sinica Nano-program and in part by the National Science Council of Republic of China (ROC) Taiwan under Contract NSC97-2112-M-001-027-MY3.

¹T. Mukai, K. Takekawa, and S. Nakamura, *Jpn. J. Appl. Phys., Part 2* **37**, L839 (1998).

²O.-H. Nam, M. D. Bremser, T. S. Zheleva, and R. F. Davis, *Appl. Phys. Lett.* **71**, 2638 (1997).

³E.-H. Park, J. Jang, S. Gupta, I. Ferguson, C.-H. Kim, S.-K. Jeon, and J.-S. Park, *Appl. Phys. Lett.* **93**, 191103 (2008).

⁴Y. J. Lee, H. C. Kuo, T. C. Lu, B. J. Su, and S. C. Wang, *J. Electrochem. Soc.* **153**, G1106 (2006).

⁵J. Xie, Ü. Özgür, Y. Fu, X. Ni, H. Morkoç, C. K. Inoki, T. S. Kuan, J. V. Foreman, and H. O. Everitt, *Appl. Phys. Lett.* **90**, 041107 (2007).

⁶Ü. Özgür, Y. Fu, Y. T. Moon, F. Yun, H. Morkoç, H. O. Everitt, S. S. Park, and K. Y. Lee, *Appl. Phys. Lett.* **86**, 232106 (2005).

⁷J. W. Lee, C. Sone, Y. Park, S.-N. Lee, J.-H. Ryou, R. D. Dupuis, C.-H. Hong, and H. Kim, *Appl. Phys. Lett.* **95**, 011108 (2009).

⁸J. L. Weyher, H. Ashraf, and P. R. Hageman, *Appl. Phys. Lett.* **95**, 031913 (2009).

⁹T. Kozawa, T. Kachi, T. Ohwaki, Y. Taga, N. Koide, and M. Koike, *J. Electrochem. Soc.* **143**, L17 (1996).

¹⁰L. Min, C. Xin, F. Hui-Zhi, Y. Zhi-Jian, Y. Hua, R. Q. Li Zi-Lan, Z. Guo-Yi, and Z. Bei, *Phys. Status Solidi C* **1**, 2438 (2004).

¹¹D. A. Stocker, E. F. Schubert, and J. M. Redwing, *Appl. Phys. Lett.* **73**, 2654 (1998).

¹²M. Albrecht, J. L. Weyher, B. Lucznik, I. Grzegory, and S. Porowski, *Appl. Phys. Lett.* **92**, 231909 (2008).

¹³K. Tadatomo, H. Okagawa, Y. Ohuchi, T. Tsunekawa, Y. Imada, M. Kato, and T. Taguchi, *Jpn. J. Appl. Phys., Part 2* **40**, L583 (2001).

¹⁴T. Mukai, D. Morita, and S. Nakamura, *J. Cryst. Growth* **189**, 778 (1998).

¹⁵S. Nakamura, *Science* **281**, 956 (1998).